Planar Broadband Dual-Linearly Polarized MEMS Steerable Antenna

Douglas A. Woten* [(1)], Magda El-Shenawee[(2)], and Steve Tung[(3)]
(1) Microelectronics-Photonics Program
(2) Electrical Engineering Department
(3) Mechanical Engineering Department
University of Arkansas
Fayetteville, Arkansas 72701
dwoten@uark.edu

Introduction

In this work we will present the fabrication process and preliminary experimental results of a MEMS steerable broadband antenna. Our previous work focused on the design of the planar broadband antennas based on the Fourpoint antenna [1]-[2]. The antenna is designed to fit on a 1cm × 1cm silicon platform with a thin benzocyclobutene (BCB) dielectric coating and operate between 4-9GHz. The modified Fourpoint antenna is simulated using ANSOFT High Frequency Structure Simulator (HFSS) and has a return loss of less than -10dB in the operating band.

Reconfigurable MEMS antennas can alter radiation, polarization and frequency characteristics by some change in the physical structure [3]-[5]. While many reconfigurable antennas focus on changing the operating frequency while maintaining the same radiation characteristics, researchers have noted the need for systems that can manipulate the radiation characteristics without changing the operating frequencies [6]. It is this problem that the proposed MEMS rotatable antenna platform seeks to address.

Device Fabrication

The proposed platform will be created using traditional bulk micromachining processes commonly used in creating MEMS accelerometers. Figure 1 depicts the envisioned final device. The device will be fabricated using a highly doped silicon <100> p-type wafer that has a double sided polish (DSP), which is necessary for double sided processes. The metallic traces used to define the antenna shape could include three layers of deposited metals such as titanium on the bottom, copper in the middle, and titanium on the top. The bottom titanium layer would serve as adhesion for the copper layer while the top titanium layer eliminates the typical rapid oxidation of the copper.

The proposed MEMS antenna can significantly capitalize on the precision thickness controls that micromachining offers. Very thin layers of titanium are necessary for adhesion and to stop oxidation while a thicker copper layer serves as the radiating element. It is important to minimize the thickness of the titanium layers since their electrical

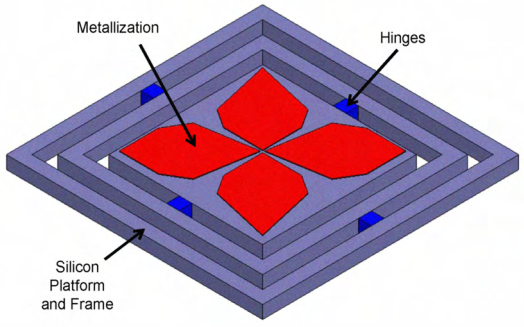

Fig 1. MEMS Antenna on a Silicon Platform

978-1-4244-3647-7/09/$25.00 ©2009 IEEE

properties are not as good as copper. The overall thickness of the three layers will affect the radiating characteristics of the device.

Fabrication of a simplified, single frame, MEMS antenna device adapted from Figure 1 consists of four major process steps outlined in Figure 2. Initially, through-holes must be etched to serve as alignment marks. The through-holes will be etched using Deep Reactive Ion Etching (DRIE) to create holes with a high depth to diameter ratio. Multiple holes are created with diameters ranging from 50-250 μm to ensure that clearly defined holes are available for alignment. These vias allow for the alignment of features on both sides of the wafer in the absence of a double-sided aligner [7].

The underside of the wafer is then etched to create a cavity below the antenna platform. This etch would ideally be performed using the DRIE or RIE processes to create vertical side-walls. The slope of the side-walls on the underside of the platform is not of critical importance, however, and a cheaper method using a wet etchant is being explored.

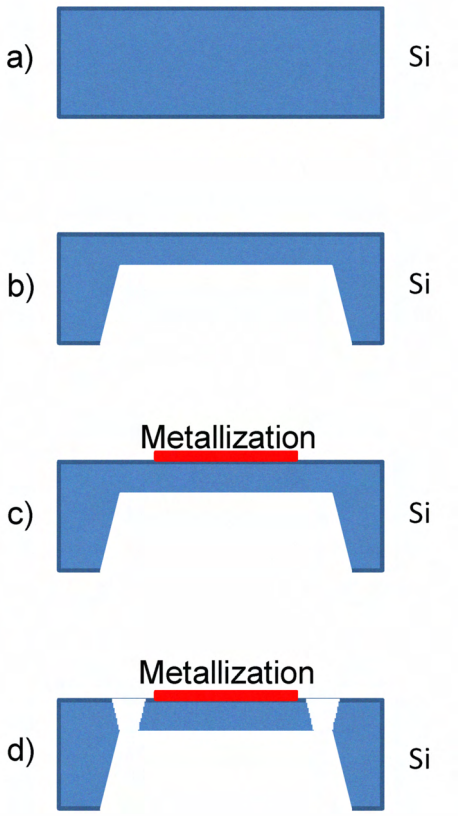

Fig. 2: Process flow of MEMS antenna platform with a) unprocessed wafer, b) backside etch, c) antenna metallization and d) platform release.

Once the cavity on the underside is created, the metallization defining the antenna is deposited. The deposition will be accomplished using the sputtering process to allow precision control over the thin layers required as detailed above. The metallization is then protected by a layer of photoresist. This is done to ensure that the tightly controlled metallization is not changed during the final etching step.

When the metallization is protected, the platform is released using DRIE. This step etches out the trenches that connect to the cavity defined by the backside etch. DRIE is used to allow for precise control over the shape of the hinges which is vital to allow accurate control of the final device and to reduce any unintentional modifications to the metallization. The structure is then anodically bonded to a glass substrate containing metallic pads. Creating a bias between the contact pads and the platform causes the hinges to deform resulting in a mechanical movement of the platform.

Packaging the MEMS antennas outlined above is important to protect the fragile platform and allow connections to external sources for excitation and measurements. Designing an appropriate package is under consideration at the University of Arkansas Low Temperature Cofired Ceramics (LTCC) lab. Ceramics are ideal for high frequency structures due to their relatively low loss tangent.

Prototype Simulation

As a proof of concept a single frame design is considered which resembles cantilever beams attached to a large proof mass. This simplified prototype MEMS platform with a single frame can be modeled theoretically by using the spring constant equation for a single cantilever beam given as:

$$K = \frac{Ewt^3}{4L^3} \tag{1}$$

Where E is Young's modulus of the beam material, t is the beam thickness, W is the beam width and L is the beam length. In this model the concentrative force is applied on the free end of the beam. This is not entirely accurate in MEMS devices where the electrostatic force is typically distributed over some length of the beam. The electrostatic force ($F = \varepsilon AV^2 / 2z^2$) between the platform and the electrode grows as a function of the distance squared. This is counteracted by the restoring spring force. As the beam gets closer to the electrode, a phenomenon called snap-down can occur in which the electrostatic force dominates the restoring force and drives the cantilever into the electrode.

Plots of the displacement of the MEMS platform modeled as two cantilevers with a large proof mass are shown in Fig. 3. In Fig 3 a double hinged design was considered with a $1cm^2$ platform, 200µm wide hinges of length 3a) 1000µm and 3b) 500µm with a clearance gap of 400µm. Theoretical calculations of (1) are consistent with the COMSOL simulations at low deflections. At large deflection angles, however, the simulations begin to diverge from the theory slightly. When the deflection begins to near the size of the clearance gap (400µm) a sharp increase in the COMSOL curve is present. This is attributed to the snap-down phenomenon.

Fig. 3 provides an estimated of the driving voltages that will be required. For the longer hinge configuration in Fig. 3a, a snap-down voltage of approximately 32V is observed. With the shorter hinge of Fig. 3b, the snap-down voltage is considerably higher at approximately 68V. Wider hinges would be expected to require higher driving voltages

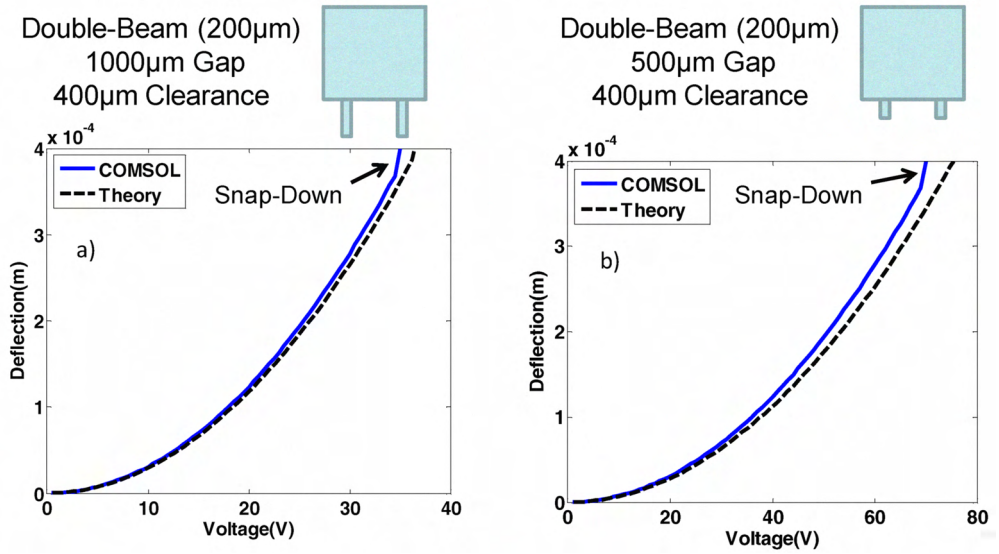

Fig. 3. Deflection vs. driving voltage for one of the prototype MEMS platforms of two different hinge lengths of a) 1000µm and b) 500µm.

while thinner hinges would require lower voltage to achieve snap-down. These voltages are considerably lower than usual for MEMS devices due to the length of the cantilever beams.

Discussion

This work will detail the fabrication processes used along with the experimentally measured results. The amount of deformation allowed by the hinges will be measured for various hinge configurations. One method to measure the deformation is using a laser beam and measuring the angle of the reflected beam. Many factors including the thickness and shape of the hinges, the position of the bias and the amount of bias induced will control the amount of mechanical movement. The degree of rotation possible is directly related to the overall size of the platform. A relatively large 1cm × 1cm platform with silicon hinges will be fabricated initially as a proof of concept. Through COMSOL simulations it is estimated that the maximum rotation angle will be on the order of 3-4°. To increase the rotation angle, polymer could provide a potential material for the hinges. The visco-elastic properties of polymer would allow for a greater degree of rotation than traditional silicon hinges.

Acknowledgements

This work was supported in part by the NSF Graduate Research Fellowship, NSF GK-12 Program and NSF Award Number ECS – 0524042.

References

[1] D. Woten, M. El-Shenawee and S. Tung, "MEMS Platform for Planar Broadband Dual-Linearly Polarized Antenna," *Proc. of the IEEE Antenna and Propagation Symposium*, San Diego, CA, USA, July 5-12, 2008.

[2] D. A. Woten and M. El-Shenawee, "Broadband Dual Linear Polarized Antenna for Statistical Detection of Breast Cancer," *IEEE Trans. Antenna and Propagation*, Vol. 56, no 11, Nov. 2008.

[3] G.H. Huff, J.T. Bernhard, "Integration of packaged RF MEMS switches with radiation pattern reconfigurable square spiral microstrip antennas," *IEEE Transactions on Antennas and Propagation, Vol. 54, Issue 2, Part 1,* Feb. 2006, pp. 464 – 469.

[4] C. Jung; M. Lee; G.P. Li, F. De Flaviis, "Reconfigurable scan-beam single-arm spiral antenna integrated with RFMEMS switches," *IEEE Transactions on Antennas and Propagation, Vol. 54, Issue 2, Part 1,* Feb. 2006, pp. 455 – 463.

[5] E. Erdil, K. Topalli, M. Unlu, O.A. Civi, T. Akin, "Frequency Tunable Microstrip Patch Antenna Using RF MEMS Technology," *IEEE Transactions on Antennas and Propagation, Vol. 55, Issue 4,* April 2007, pp. 1193 – 1196.

[6] N. Haridas, A.T. Erdogan, T. Arslan, M. Begbie, "Adaptive Micro-Antenna on Silicon Substrate," *First NASA/ES Conference on Adaptive Hardware and Systems, (AHS 2006),* 15-18 June 2006, pp. 43 – 50.

[7] L. M. Roylance and J. B. Angell, "A Batch-Fabricated Silicon Accelerometer," *IEEE Trans. Electron Devices*, Vol. 26, no. 12, Dec. 1979.